INDC   INTERNATIONAL NUCLEAR DATA COMMITTEE

SPECTRA OF INELASTICALLY SCATTERED NEUTRONS

WITH AN INITIAL ENERGY OF 14.1 MeV

AND NUCLEAR LEVEL DENSITY

O.A. Sal'nikov, N.I. Fetisov, G.N. Lovchikova
G.V. Kotel'nikova, V.B. Anufrienko, B.V. Devkin
Fiziko-Energeticheskij Institut
Obninsk, Kaluga Region, USSR

Translated by the IAEA

SPECTRA OF INELASTICALLY SCATTERED NEUTRONS

WITH AN INITIAL ENERGY OF 14.1 MeV

AND NUCLEAR LEVEL DENSITY

O.A. Sal'nikov, N.I. Fetisov, G.N. Lovchikova
G.V. Kotel'nikova, V.B. Anufrienko, B.V. Devkin
Fiziko-Energeticheskij Institut
Obninsk, Kaluga Region, USSR

Translated by the IAEA

February 1989

The present paper on the measurement of the spectra of secondary neutrons formed by the interaction of 14.1 MeV neutrons with the nuclei of the 14 elements: Be, Na, Mg, S, K, Ca, Sr, In, Sb, I, Cs, Ce, Ta, Hg, is a continuation of Ref. [1], where similar measurements are given for 23 elements.

We thus have data on the secondary neutron spectra for the nuclei of 37 elements distributed fairly evenly over the range of mass numbers A from 9 to 209.

The availability of such systematic data permits a more comprehensive idea to be gained as to the dependence of the nuclear temperature and the nuclear level density parameter on the mass number A, as to the mechanism of the (n,n') reaction and as to the spectra of neutrons from the (n,2n) reaction. A comparison of the results from the present paper and Ref.[1] with nuclear temperature measurement and nuclear level density parameter data obtained at lower excitation energies allows the dependence of these two values (T and a) on energy to be established.

The geometry of the experiment, the apparatus used to obtain the present results and its characteristics are described in Ref.[1].

The scatterers were ring-shaped, and no more than 15 mm thick; the Na, K, I, Cs and Hg were in containers.

In processing the measurement results (recorded spectra), a correction was introduced, as before, for sprectrometer dead time and to take into account activation of samples, the effect of the scatterer on monitor counts, the cosmic-ray background and noise in the photo-multiplier, for different measuring times of both effect and background. To determine the nuclear temperature, as in Ref.[1], graphs of $\ln[N(E)/E]$ were plotted from the experimentally measured spectra of scattered neutrons $N(E)$, and, where necessary, graphs of $\ln[N(E)/E^{5/11}]$ (see Figs 1, 2, 3).

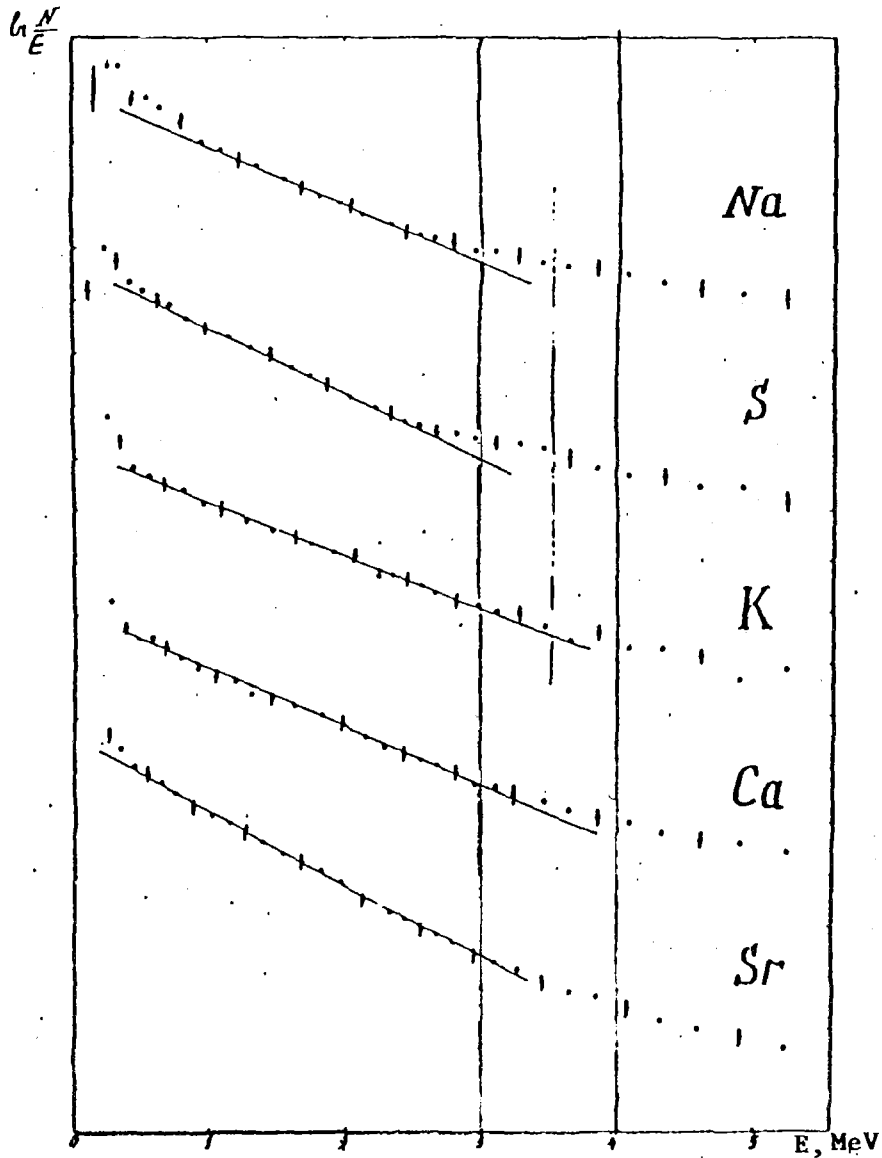. Table 1 gives the values for the temperatures T_{eff} and T_1.

Fig. 1. Graph of $\ell_n \dfrac{N(E)}{E}$ as a function of the energy of inelastically scattered neutrons for sodium, sulphur, potassium, calcium and strontium.

T_{eff} is the nuclear temperature as determined from the total neutron spectrum for the reactions (n,n') and (n,2n). For this, the linear part of the graph of lnN(E)/E from 0.4 to 2-3.5 MeV was used.

T_1 is the temperature characterizing the excitation of the target nucleus after emission of the first neutron. For single-isotope elements and multi-isotope nuclei with similar binding energy values for the neutron in the target nucleus, T_1 was determined using the second linear portion of the graph of lnN(E)/E. For multi-isotope nuclei with different binding energies
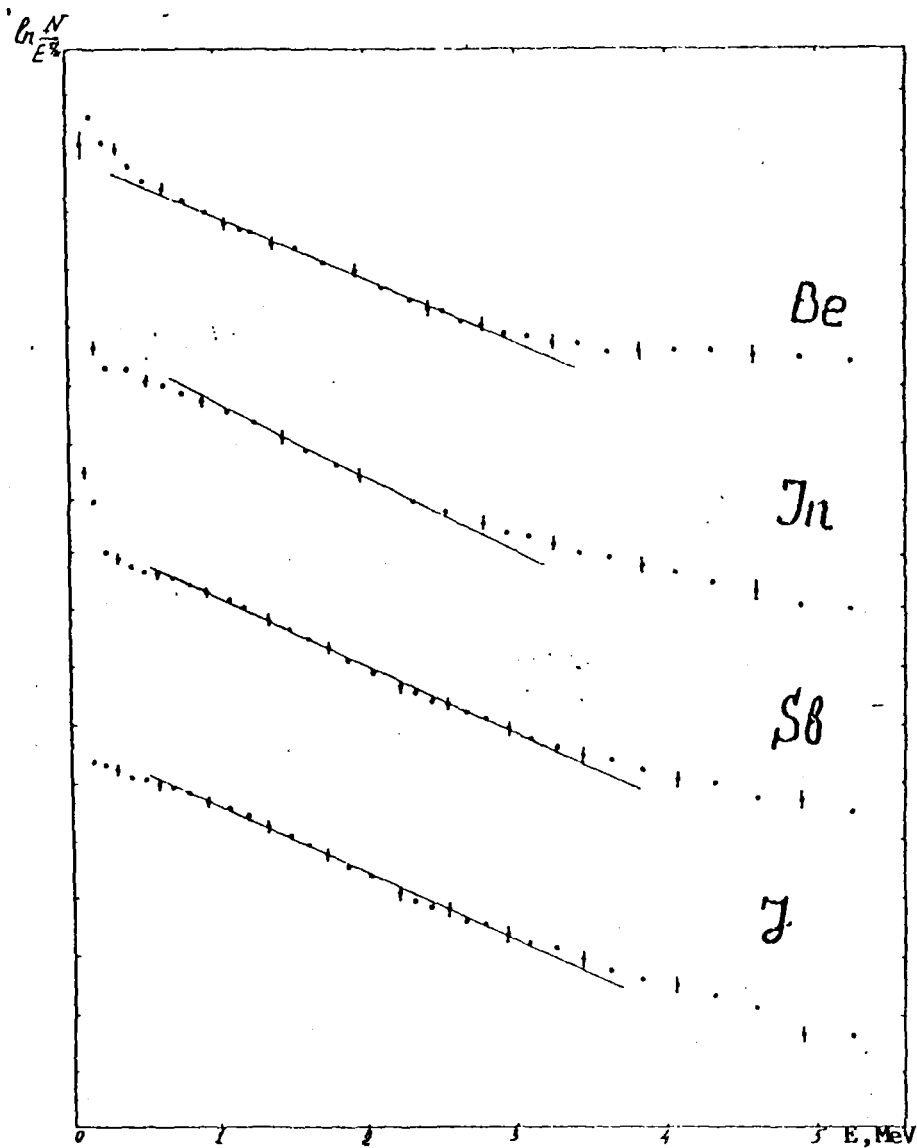
4

Fig.2. Graph of $\ln N(E)/E^{5/11}$ as a function of the energy of inelastically scattered neutrons for beryllium, indium, antimony, iodine.

for the neutron in the target nucleus, T_1 was determined using the Le Couteur method.

In addition to the results of the present study, temperatures measured previously by ourselves and by other authors, are also given. For light elements such as C, Mg, Al, S, K, Ca, the idea of temperature is not entirely applicable, but it was calculated for the purpose of comparison with the data from other studies, and also for the sake of being systematic.

The nuclear temperature values obtained allowed the nuclear energy-level density parameters to be determined assuming a Fermi-gas-type nucleus
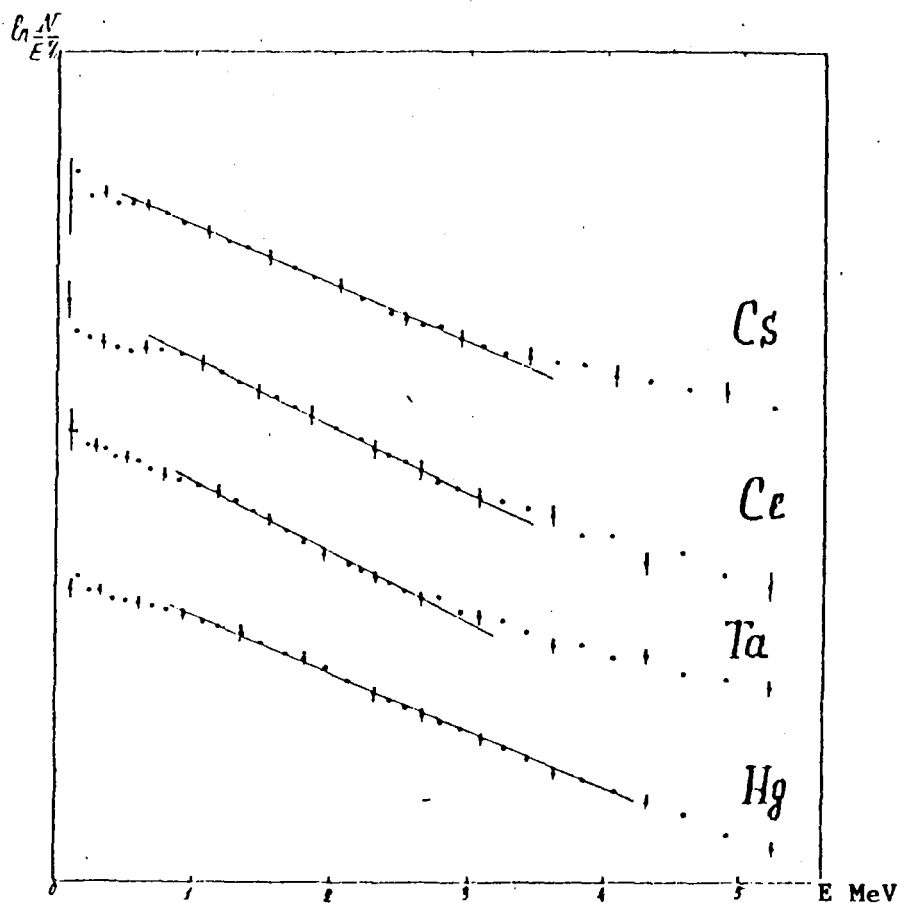
5

Fig. 3. Graph of $\ln N(E)/E^{5/4}$ as a function of the energy of inelastically scattered neutrons for caesium, cerium, tantalum and mercury.

DASTAR — P0008

FEhI-30

Table 1

A	Element	Results of this study			Results of other studies		
		T_{eff}	T_1 (Le Couteur)	T_1	E_o	T_{eff}	T_1 (Le Couteur)
9	Be	0,71±0,07	1,02±0,10		14	0,7±0,07 [2]	
12	C	0,55±0,04			14,0	0,82±0,08 [2]	
					14,8	1,04±0,11 [3]	
					14,0	0,93±0,14 [4]	
23	Na	0,89±0,10		2,02±0,21			
24	Mg	1,03±0,10 *			14	0,98±0,02 [2]	
27	Al	0,91±0,05			14,0	1,19±0,09 [2]	
					14,0	1,01±0,10 [3]	
					14,8	1,06±0,16 [4]	
28	Si	0,68±0,05					
31	P	0,74±0,07		1,91±0,20			
32	S	0,79±0,08		1,89±0,19			
39	K	1,04±0,10					
40	Ca	0,94±0,09					
48	Ti	0,82±0,05 *		1,46±0,09			

6

1	2	3	4	5	6	7	8
51	V	0,83±0,05		1,18±0,07			
52	Cr	0,85±0,05 ×		1,40±0,03			
55	Mn	0,78±0,04 ×		1,45±	14	1,08±0,09 [5]	
56	Fe	0,75±0,04		1,45±0,07	14,0	0,70±0,07 [2]	
					14,0	0,76±0,08 [3]	
					14,0	0,80±0,08 [6]	
59	Co	0,74±0,04		1,39±	14,0	0,97±0,09 [5]	
58	Ni	0.72±0,03		1,45±0,06			
64	Cu	0,66±0,02		1,27±0,04	14,0	0,76±0,05 [2]	
					14,0	0,77±0,08 [3]	
					14,8	0,82±0,12 [4]	
65	Zn	0,69±0,04		1,28±0,06	14,0	0,73±0,07 [3]	
79	Se	0,63±0,06	0,98±0,10				
88	Sr	0,72±0,05		1,28±0,09			
91	Zr	0,71±0,04		1,17±0,06			
93	Nb	0,66±0,03		1,11±0,06			
96	Mo	0,60±0,04	0,91±0,06		14	0,65±0,06 [2]	0,90±0,04 [7]
112	Cd	0,61±0,04			14,0	0,62±0,05 [2]	
			0,91±0,06		14		0,85±0,04 [7]
115	In	0,62±0,04	0,91±0,06				
119	Sn	0,68±0,04			14,0	0,56±0,05 [3]	
					14,8	0,62 [4]	
			1,02±0,06		14		0,83±0,04 [7]
122	Sb	0,62±0,04			14	0,6±0,06 [2]	
			0,92±0,06		14,0		0,89±0,04 [7]
128	Te	0,69±0,07	1,06±0,11		14		0,96±0,05 [7]
127	J	0,65±0,04			14	0,81±0,08 [5]	
			0,88±0,06		14		0,89±0,04 [7]
133	Cs	0,68±0,06	1,00±0,07				
140	Ce	0,66±0,04	0,89±0,06		14		0,90±0,04 [7]
181	Ta	0,60±0,04	0,86±0,06				
184	W	0,61±0,04	0,84±0,05		14,0	0,62±0,08 [2]	
201	Hg	0,72±0,04			14	0,6 ±0,05 [2] *	
			0,96±0,06		14,7		0,8 [8]
					14		0,98±0,05 [7]
					14,5		0,87±0,05 [9]
207	Pb	0,93±0,06			14,0	0,73±0,05 [2]	
					14,8	0,75±0,12 [4]	
					14,0	0,76±0,08 [3]	
					14,0	0,75±0,08 [6]	
					14	0,8 [10]	
			1,45±0,09		14,7		0,9 [8]
					14		1,28±0,07 [7]
					14,5		1,06±0,03 [9]
209	Bi	0,92±0,06			14,0	0,95±0,10 [3]	
					14,0	0,9±0,08 [2]	
					14	0,9 [10]	
					14	0,95±0,09 [5]	
			1,42±0,09		14,7		1,05 [8]
					14,0		1,26±0,06 [7]
					14,0		1,05 [11]

* Hg²⁰¹

7

model. The level density parameters a, a' and a'' were determined using the following formulae:

$$a = \frac{E^*}{T_1^2}$$ (1)

$$a' = \left(\frac{1}{T_1} + \frac{5}{4\bar{E}^*}\right)^2 \bar{E}^*$$ (2)

$$a'' = \left(\frac{1}{T_1} + \frac{2}{\bar{E}^*}\right)^2 \bar{E}^*$$ (3)

where $\bar{E}^* = E_o - 2T_1$ is the mean excitation energy of the target nucleus. The density coefficient values, calculated on the basis of the temperatures determined by ourselves, are given in Table 2. In addition, the values for a and a'' from Ref. [12] are given for neutrons with an initial energy level of 7 MeV. As may be seen, they agree with our results to within the measurement error. Table 3 gives level density coefficient values taking into account pairing energy – a_p, a_p' and a_p''; these were determined using formulae (1), (2) and (3), respectively, replacing $\bar{E}^*$ by

$U = E_o - 2T_1 + P_Z + P_N$. The Table also presents the values for these coefficients given in Ref. [12] for neutrons with an initial energy of 7 MeV, and values for a_p' obtained from an analysis of neutron resonance data [13].

The data in Table 3 show the nuclear level density parameters rising with the mass number A, as required by the Fermi-gas model. Near closed shells, troughs are observed in the rise of the level density parameter, in line with the shell model's prediction that the nuclear level density parameter will fall sharply for magic or near-magic nuclei. The agreement, within the measurement error, between the coefficients obtained in this study and the coefficients given in Refs [12] and [13] shows that the Fermi-gas model is applicable in the majority of cases. Figure 4 gives the Newton curve for level density coefficients for different values of A, and our data for a_p'. Figure 5 plots the dependence of the cross-section for the inverse process $\sigma_i(E,E^*)$ on E^* for In. The values for the cross-section were

8

Table 2

Element	Results of this study a (MeV)$^{-1}$	a''(MeV)$^{-1}$	Results from Ref.[12], $E_0 = 7$ MeV a (MeV)$^{-1}$	a''(MeV)$^{-1}$
Be				
C	43,3	50,4		
Na	2,5	4,8		
Mg	11,4	15,6		
Al	15,2	19,8	5,5	10,5
Si	27,7	33,9		
P	2,8	5,3		
S	2,9	5,4		
K	11,1	15,3		
Ca	13,8	18,4		
Ti	5,2	8,3		
V	8,4	12,2	6,4	11,7
Cr	5,8	9,0		
Mn	5,3	8,3	5,9	9,8
Fe	5,3	8,4	5,7	10,7
Co	5,9	9,1		
Ni	5,3	8,1		
Cu	8,0	11,6	8,7	14,6
Zn	7,0	10,5		
Se	12,7	16,9	15,0	22,1
Sr	7,0	10,5	8,4	14,2
Zr	8,6	12,4		
Nb	9,6	13,6	16,7	24,2
Mo	14,8	19,5		
Cd	14,8	19,5		
In	14,8	19,6	18,8	26,6
Sn	11,6	15,9		
Sb	14,5	19,2	17,4	24,9
Te	10,7	14,7		
I	15,9	20,8	16,1	23,5
Cs	12,1	16,4		
Ce	15,6	20,4	16,2	23,5
Ta	16,7	21,7	22,1	30,4
W	17,5	22,6	24,0	32,6
Hg	13,2	17,7		
Pb	5,3	8,5	6,1*	11,2*
Bi	5,6	8,7	4,5	9,1

*) For Pb 206

calculated using the formula:

$$G_i \left(E, E^* \right) = \frac{N(E)}{E \exp 2(1/4, 8 E^*)^{1/2}} \tag{4}$$

Table 3

Ele-ment	Results of present study $E_0 = 14.1$ MeV			Results from Ref.[12] $E_0 = 7$ MeV		Results from Ref.[13]
	a_ρ (MeV)$^{-1}$	$a_\rho{}'$ (MeV)$^{-1}$	$a_\rho{}''$ (MeV)$^{-1}$	a_ρ (MeV)$^{-1}$	$a_\rho{}''$ (MeV)$^{-1}$	
P	2,3	4,0	4,9			
S	1,9	3,5	4,6			3,5
K	10,1	12,7	14,3			
Ca	9,7	12,7	14,4			
Ti	3,9	5,4	7,1			6,5
V	7,4	9,8	11,2	4,6	10,1	5,7
Cr	4,4	6,0	7,7			7,0
Mn	4,9	6,7	8,0			7,0
Fe	4,0	5,9	7,3	2,6	8,5	6,9
Co	5,1	6,8	8,4			5,8
Ni	4,0	5,9	7,3			6,2
Cu	7,0	9,3	10,7	6,4	12,4	8,0
Zn	5,5	7,4	9,1			8,2
Se	9,9	12,2	14,4	8,0	15,7	12,0
Sr	5,2	7,3	8,8	4,6	11,0	8,0
Zr	7,2	9,6	11,0			9,4
Nb	9,1	11,8	13,1	14,9	22,5	10,7
Mo	12,4	15,1	17,3			11,0
Cd	12,0	14,7	16,8			16,6
In	13,6	16,5	18,4			16,0
Sn	9,3	11,8	13,7			13,7
Sb	13,1	15,9	17,8	13,5	21,3	16,2
Te	8,9	11,1	13,0			16,1
J	14,5	17,5	19,4	12,8	20,3	16,5
Cs	11,2	13,8	15,6			15,5
Ce	13,0	15,9	17,8	11,3	18,9	14,0
Ta	15,9	19,0	20,9	18,5	27,0	20,5
W	14,7	19,0	19,9	15,4	24,5	20,0
Hg	11,4	14,1	15,9			15,4
Pb	4,7	6,7	7,8	4,5*	9,9*	7,5
Bi	5,2	7,2	8,3	3,7	8,5	7,8

x) For Pb 206

Figure 5 shows a rise in the high excitation energy region which may be caused by the presence of neutrons from the (n,2n) reaction; a sharp rise in the inverse process cross-section can also be seen in the low excitation energy region, which is characteristic for direct processes.
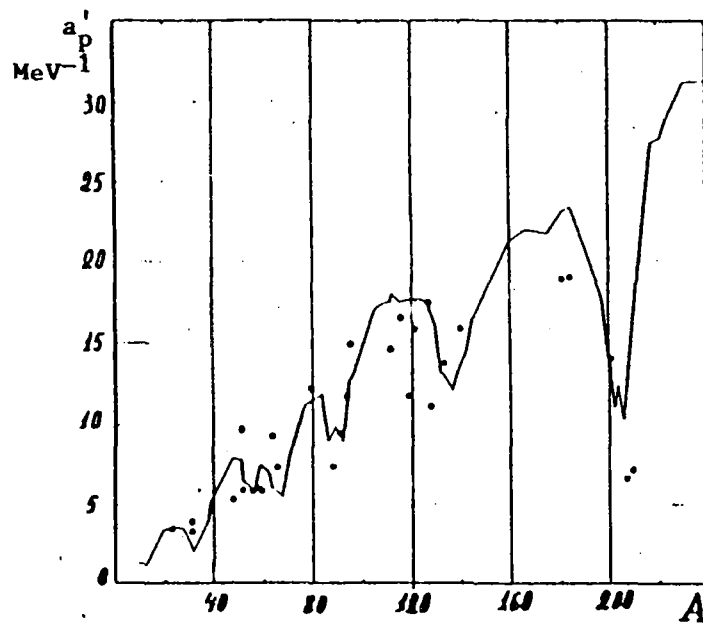
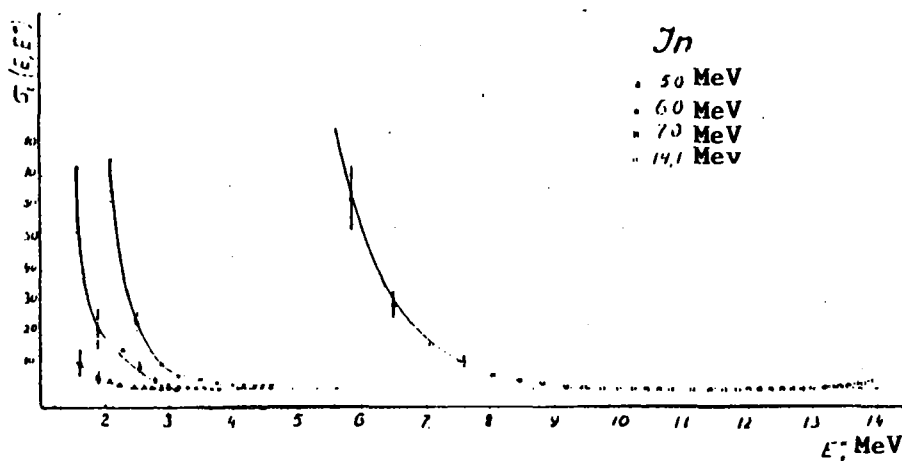**Fig. 4.** Dependence of total level density coefficients a_p' on atomic weight.

Fig. 5. Dependence of inverse process cross-section σ_i (E, E^+) on excitation energy E^*.

Figure 6 shows secondary neutron spectra for the (n,2n) reaction, which represent the difference between the full spectrum and the spectrum described by the equation:

$$N(E) = const \cdot E \exp\left(- \frac{E}{T_i}\right),$$

where T_1 are the values found for the temperatures of the residual target nucleus.

11
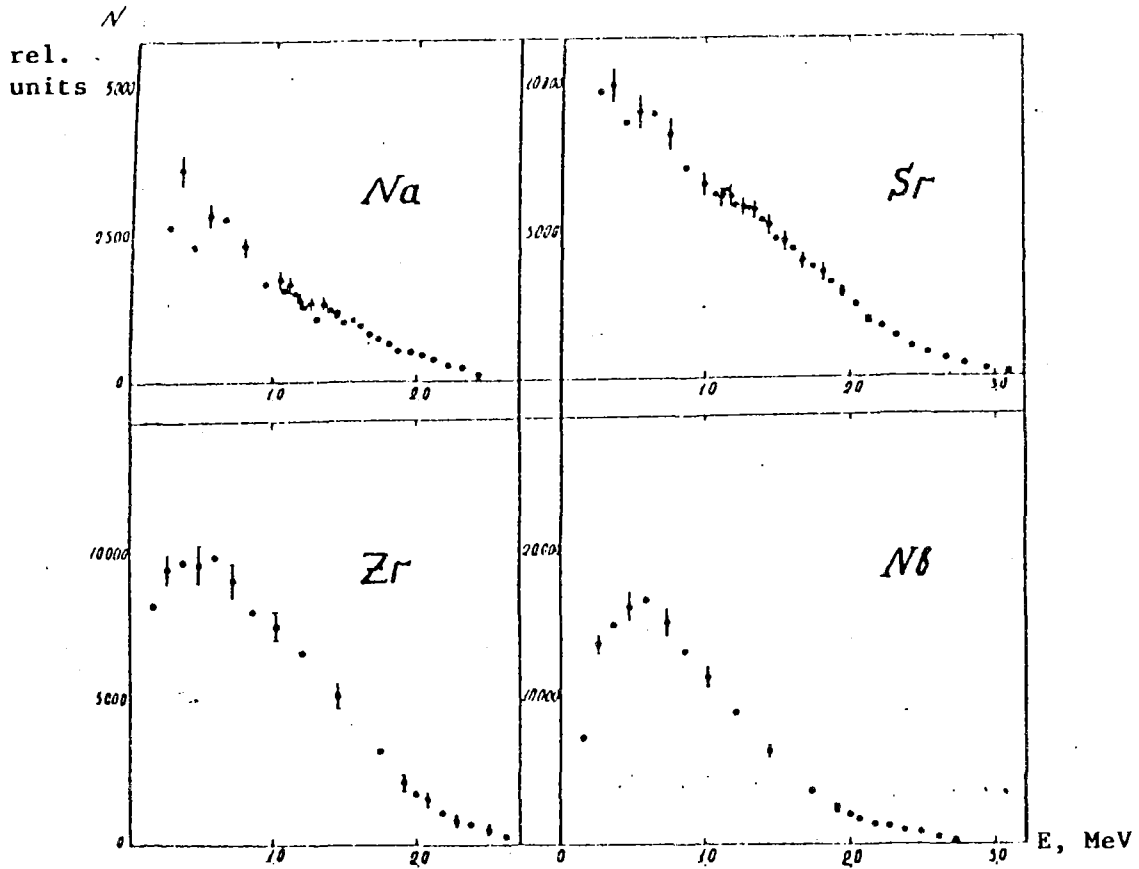
Fig. 6. Spectra of secondary neutrons from the (n,2n) reaction for sodium, strontium, zirconium and niobium.
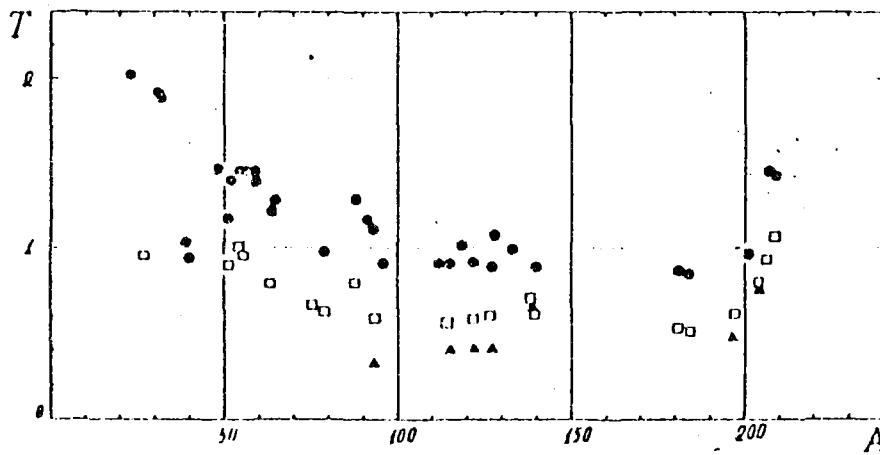

Fig. 7. Temperature change as a function of atomic weight.

The nuclear temperature values obtained allowed their dependence on the mass number A to be determined. According to the Fermi-gas model of the nucleus, the temperature of the nucleus, corresponding to the excitation energy determined, should decrease as A increases, since the excitation energy will be distributed over a larger number of nucleons as A increases. The

equation of state for a Fermi gas takes the form:

$$E^{*} = aT^{2}$$

(5)

where a is the level density coefficient which is proportional to the number of particles in the nucleus.

In the first approximation

$$a = \alpha A$$

(6)

where $\alpha \simeq 0.03-0.07$ is assumed. From Eqs (5) and (6) it follows that:

$$T = \sqrt{\frac{E^{*}}{\alpha}} \cdot \frac{1}{\sqrt{A}}$$

(7)

Figure 7 presents the results of the present work and data obtained by previously by the authors [1] and by Thomson [12] for neutrons with an energy of 7 MeV. The figure shows a reduction in temperature as A increases, except for magic nuclei. The temperature values for light nuclei do not follow the general pattern of the dependence on A.

The dependence of the temperature on the mass number can be determined more correctly determined for the identical excitation energy of the residual nucleus. The temperatures determined in the experiment relate to different
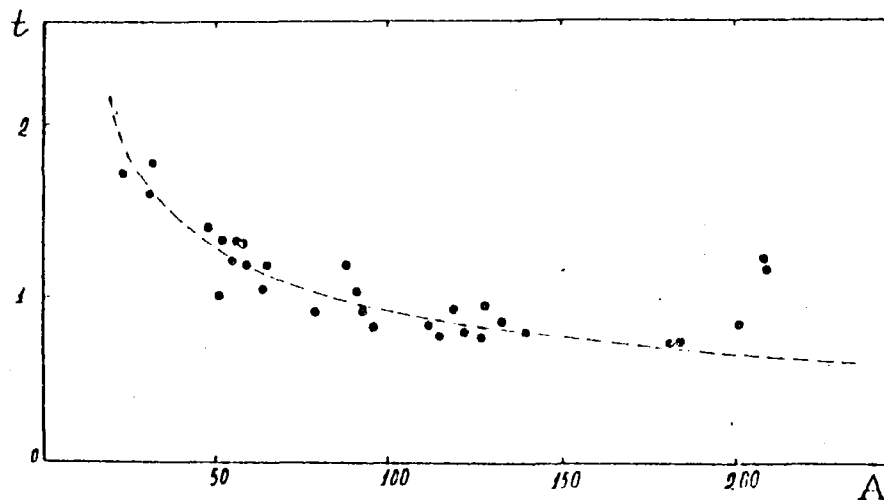

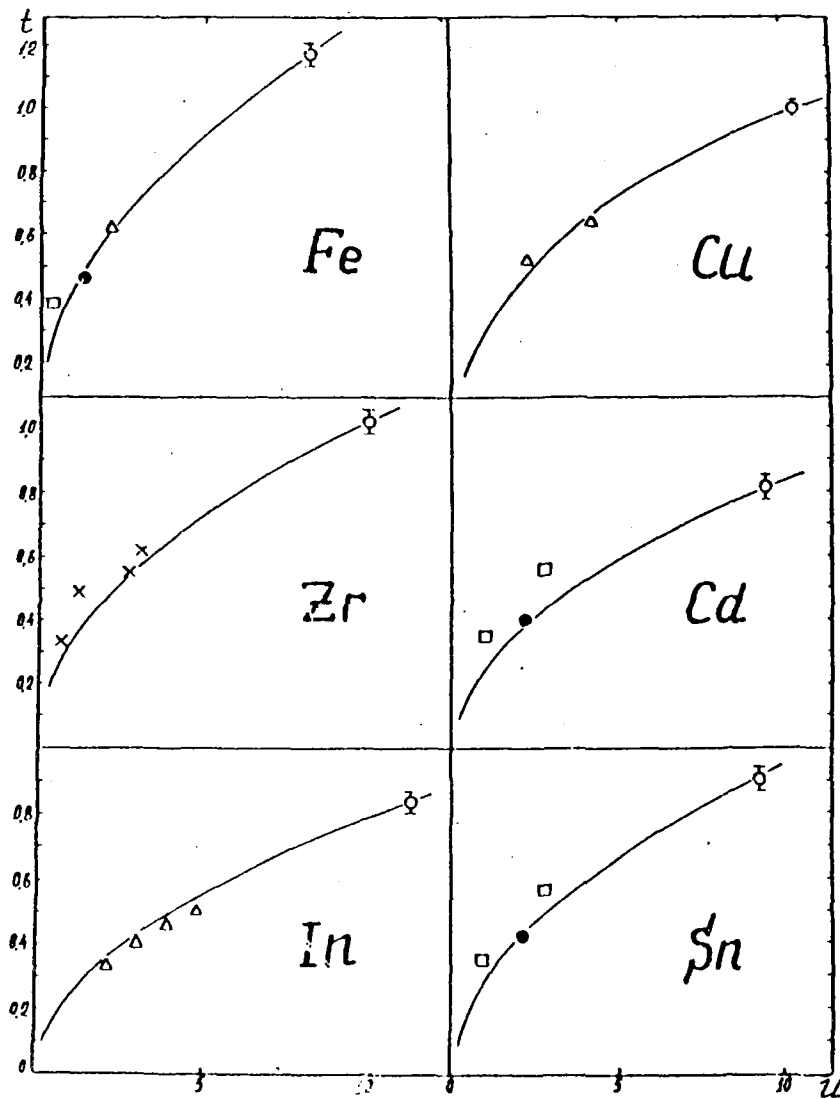Fig. 8. Dependence of thermodynamic temperature on atomic weight.

Fig. 9. Dependence of thermodynamic temperature on excitation energy U for iron, copper, zirconium, cadmium, indium and tin.

Δ - Thomson [12] , ● - Seth [14] , □ - Ewing [15] ,
× - Buccino [16]   ▲ - Levin, Cranberg [17] ,   ○ - present study

excitation energies, though the energy of the initial neutrons was the same. Figure 8 shows the thermodynamic temperatures as a function of A, calculated using the formula

$$t = \sqrt{\frac{U}{a_f'}}$$ (8)

for an excitation energy U = 10 MeV. This level was chosen because, for the majority of nuclei studied, the excitation energy U calculated using the formula

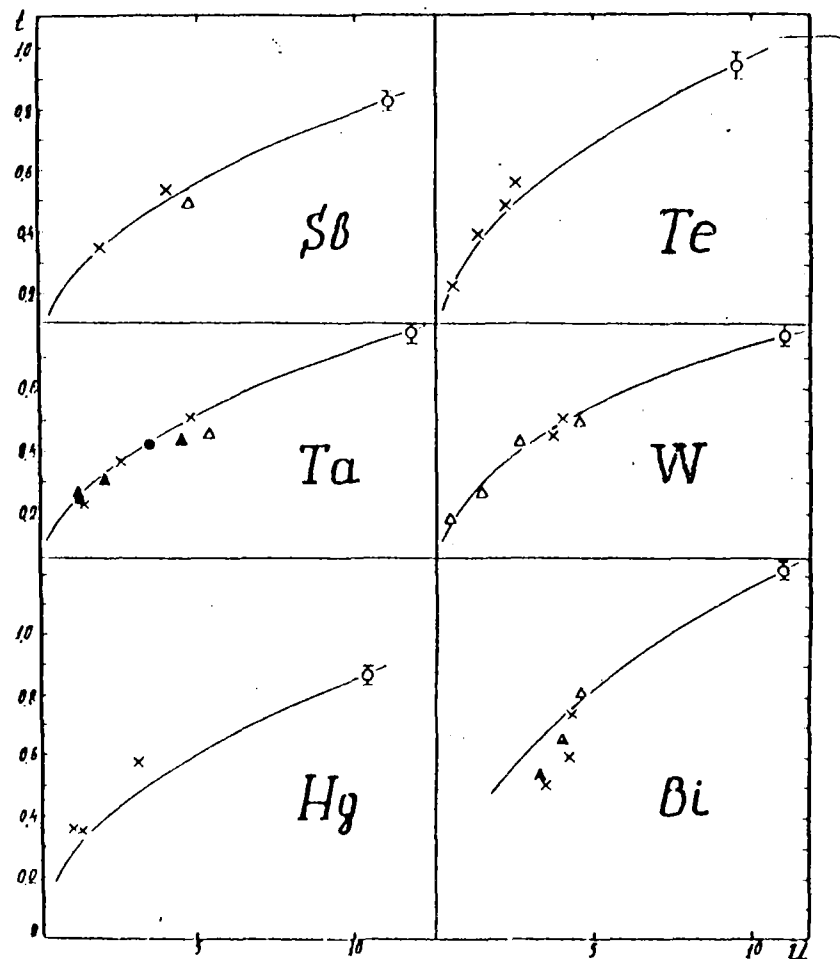$$U = 14,1 - 2T_i + P_z + P_N$$ (9)

14

Fig. 10.   Dependence of thermodynamic temperature on excitation
energy U for antimony, tellurium, tungsten, mercury, tantalum
and bismuth. Symbol key as for Fig. 9.

proved to be ≃ 10 MeV. Values for P_Z and P_N were taken from Ref. [13].

The dotted curve in the diagram is a theoretical curve calculated using

formula (5) for an excitation energy of 10 MeV where α = 0.12. The high

level of agreement between the temperatures t predicted theoretically and the

experimental data for an excitation energy of 10 MeV is good evidence in

support of the Fermi-gas model of the nucleus. Figures 9 and 10 show

thermodynamic temperatures taking into account pairing energy and the

contribution of the (n,2n) reaction for various excitation energies. To

analyse the dependence of the temperature on the excitation energy of the

nucleus, elements were chosen for which the temperatures had already been

determined for several neutron energy values. In addition to the experimental

points, the graphs show curves for the dependence of temperature on excitation
energy as given by the Fermi-gas model, and as determined using Eq. (8).

Conclusion

The results of this study allow the following conclusions to be drawn:

1. For medium and heavy nuclei at an excitation energy of 10 MeV, it
    is perfectly possible to describe the majority of inelastically
    scattered neutron spectra by means of the nuclear temperature;

2. The linear dependence of lnN/E on E shows that scattering
    accompanied by the formation of a compound nucleus amounts to at
    least 80%, at an initial neutron energy of 14.1 MeV. These
    results also show that direct interaction plays a significant role
    for those neutrons which lose only a small amount of energy in the
    scattering process;

3. The observed change in nuclear temperature with excitation energy
    shows a high level of agreement with the Fermi-gas model in the
    2-10 MeV excitation energy range . The change in nuclear
    temperature with mass number also agrees well with the Fermi-gas
    model;

4. A rise in level density is observed as the mass number increases,
    except for nuclei close to having closed shells, where the level
    density drops significantly. These results agree both
    qualitatively and quantitatively with the α parameter values
    obtained from experimental data on the mean distances between
    neutron resonances. A high level of agreement with the
    a parameter values obtained for inelastic scattering of neutrons
    with an initial energy of 7 MeV is observed.

5. The measurement of the spectra of inelastically scattered neutrons
    with a low neutron detection threshold allowed the contribution to
    the scattering process of neutrons from the (n,2n) reaction to be

16

taken into account correctly, and the spectra of secondary

neutrons from this reaction to be obtained.

REFERENCES

[1]   ANUFRIENKO, V.B., DEVKIN, B.V. et al., FEhI Preprint No. 4 (1965).
[2]   ZAMYATNIN, Yu.S. et al., At. Ehnerg. 3 12 (1957) 540.
[3]   GRAVIS, E.R., ROSEN, L., Phys. Rev. 89 (1953) 343.
[4]   O'NEIL, G.K., Phys. Rev. 95 (1954) 635 and 1235.
[5]   ARNOLD, R.T., BUNJARD, G.B., BAPS 5 (1960) 104.
[6]   SUKHANOV, B.I., RUKAVISHNIKOV, V.G., At. Ehnerg. 11 (1961) 398.
[7]   HUBER et al., Phys. Lett. 5 3 (1963) 202.
[8]   HUBER, P., NIKLAUS, P., WAGNER, R., Helv. Phys. Acta 33 (1960) 560.
[9]   NIKLAUS, P. et al., Helv. Phys. Acta 34, 5 (1961) 520.
[10]   WHITMORE, B.G., DENNIS, G.E., Phys. Rev. 84 (1951) 296.
[11]   ROSEN, L., STEWART, L., Phys. Rev. 107 3 (1957) 824.
[12]   THOMSON, D.B., Phys. Rev. 129 4 (1963).
[13]   MALYSHEV, A.V., Zh. Ehksp. Teor. Fiz. 45 2 (8) (1963) 316.
[14]   SETH, K.K., WILENZICK, R.M., GRIFFY, T.A., Phys. Lett. 11 4 (1964) 308.
[15]   EWING, R.J., BONNER, T.W., BAPS 6 (1961), 149.
[16]   BUCCINO, S.G., HOLLANDSWORTH, C.E., LEWIS, H.W., BEVINGTON, P.R., Nucl.
       Phys. 60 1 (1964) 17.
[17]   LEVIN, J.S., CRANBERG, L., BAPS 2 (1957) 219.